



Direct Aqueous Mineralization of Industrial Waste for the Production of Carbonated Supplementary Cementitious Materials

Francesca Bonfante¹, Giuseppe Ferrara¹ , Pedro Humbert² ,
Jean-Marc Tulliani¹ , and Paola Palmero¹  

¹ Politecnico di Torino, Torino, Italy
paola.palmero@polito.it

² Innovation Centre for Sustainable Construction, CRH, Amsterdam 1083 HL, Netherlands

Abstract. In the steelmaking process, electric arc furnace (EAF) is regarded as a green production route, as it essentially uses ferrous scraps instead of virgin raw materials. In addition, the alkaline composition of the slag derived from the EAF production makes it suitable for carbonation treatment, and specifically for the permanent storage of CO₂ through the implementation of the mineralization process. Therefore, in this study, EAF slag carbonation is performed in a slurry configuration, at room temperature and ambient pressure, in order to assess the CO₂ storage potential under minimized energy consumption conditions. Specifically, the slurry was prepared at a liquid-to-solid ratio of 3; CO₂ with a partial pressure of 99.9% was fluxed into the slurry at 25 °C under the pressure of 1 bar with a flowrate of 150 L/h, and reaction time of 1 h. Moreover, in order to investigate the reproducibility of the mineralization process, three tests under the same conditions were replicated. The carbonation efficiency was estimated to be around 32%, and the results achieved were compared to previous literature studies. This research confirms that direct aqueous carbonation is a valuable method for inducing mineralization in powdered materials. Future investigations will be aimed at assessing the potential of the carbonated slag to act as supplementary cementitious material by partially substituting clinker binders in cement-based manufactures.

Keywords: Electric Arc Furnace slag · Wet carbonation · Industrial waste · Carbonation efficiency · Supplementary Cementitious Material

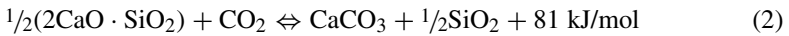
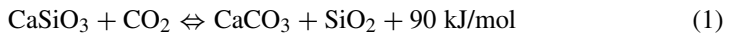
1 Introduction

The Net Zero Emissions by 2050 Scenario estimated that the global average clinker-to-cement ratio should decrease by 1.0% per year, while it has currently increased by 1.6% per year [1]. Clinker production is directly responsible of up to 60% of the cement industry CO₂ emissions, since the process involves limestone decomposition into CaO and CO₂ [2].

Together with cement production, crude steel production, and, consequently, steel slag production have been increasing in the last twenty years [3]. Electric arc furnace

(EAF) allows the production of steel from the metal scrap, accounting as a ‘green’ steel solution. In 2018, the European production of EAF steel amounted to 69 million tons [4], while EAF steel slag was reported to be 4 million tons [5]. EAF slag can be distinguished between EAF C, from carbon steel production, and EAF S from stainless steel production. The EAF C slag generation has been calculated at three times EAF S slag [5]. Originally, steelmaking slags were identified as waste and disposed to landfill, where their alkaline leachates were to be managed. Nowadays, steel slag is qualified as a by-product thanks to its promising characteristics, with perspectives to be placed on the market and to be reused in sectors where it is most suitable, without undergoing “end of waste” operations. In the construction and road sectors, it is mainly used as hydraulically bound layer and aggregate for concrete and bituminous mix, while its use as supplementary cementitious material (SCM) is currently under investigation [6]. The partial substitution of clinker-based cement with steel slag is also standardised by UNI EN 197/1 [7]. Huijgen et al. [8, 9] have determined that fresh EAF steel slags can contain three major phases of calcium: portlandite, calcium-iron silicates, and calcium-iron oxides. This alkaline composition makes them suitable for treatments such as carbonation, and specifically for the permanent storage of CO₂ through the implementation of the mineralization process.

In general, the accelerated carbonation reaction can be carried out in dry or wet conditions. The aim is to accelerate the natural weathering of silicate minerals, allowing them to react with CO₂ in order to form stable products, in particular calcium and magnesium carbonates. For mineral silicates, as in the case of compounds present in EAF slag, the reaction kinetics are reported in Eqs. (1) [10] and (2) [11].



According to different studies [12], the selection of a wet route for the carbonation of silicates can provide a higher contact frequency between dissolved CO₂ and calcium ions with respect to the dry route, performed in absence of water.

Among the aqueous mineralization processes, slurry carbonation emerged as the most promising one [13]. However, due to the wide range of adopted boundary conditions (i.e. pressure, temperature) and to the non-homogeneity in the properties of the raw material, results from the literature are not always consistent [13, 14]. This variability in the data makes it difficult to define both the actual CO₂ storage potential of the material and the energy consumption associated to the process and highlights the need of further investigation.

To this purpose, in this study, slurry carbonation of EAF-C slag (hereinafter referred to as EAF slag) is done at room temperature and ambient pressure conditions in order to assess the CO₂ storage potential under minimized energy consumption conditions. Moreover, in order to investigate the reproducibility of the mineralization process, tests are replicated, and the variability of the results is discussed. A comparison with main results from the literature is provided as well.

2 Materials and Methods

2.1 Material

The slag used in this research was produced by carbon steelmaking process and was collected downstream the Electric Arc Furnace treatment unit. The initial granulometry was in the range 0–6 mm, so that a grinding treatment was performed (firstly with a Jaw Crusher and subsequently with a Jet Mill), providing the particle size distribution (as determined by laser granulometry, Malvern Mastersizer 3000 AERO S) depicted in Fig. 1. The D_{10} , D_{50} and D_{90} values, determined by the cumulative curve distribution, were 1.51 μm , 9.36 μm and 24.1 μm , respectively, while the maximum grain size detected was 50.4 μm .

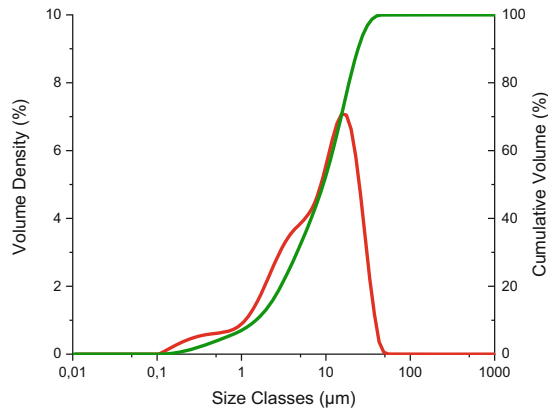


Fig. 1. Cumulative and Density granulometric curves of the milled material.

The mineralogical composition of the material was investigated through X-ray diffraction analysis (XRD, Empréan Malvern Panalytical) with $\text{Cu K}\alpha$ wavelength radiation (0.15406 nm) and operating at 40 kV and 40 mA.

The elemental composition was determined by X-ray fluorescence (XRF Rigaku, Supermini200). Iron, calcium, silicon, aluminium and manganese, all expressed as oxides, resulted as the most abundant elements in the powder (Table 1).

Table 1. EAF slag chemical composition.

Element	Fe_2O_3	CaO	SiO_2	Al_2O_3	MgO	MnO	TiO_2	P_2O_5	SO_3	Other	LOI-Flux
(%)	29.5	27.0	16.3	10.4	5.2	4.6	0.6	0.5	0.3	0.8	4.8

From the chemical composition of the material, it is possible to calculate the theoretical maximum extent of carbonation, ThCO_2 , according to Eq. (3). This equation is based on the Steinour formula [15], but it is adapted by Huntzinger et al. [16] to generic

materials other than mortars and concrete. The assumption is that all of the CaO (except that already bound in CaSO₄ and CaCO₃) will form CaCO₃, MgO will form MgCO₃, and Na₂O and K₂O (less that bound in sylvite, KCl) will form Na₂CO₃ and K₂CO₃.

$$\begin{aligned} \%ThCO_2 = & 0.785(\%CaO - 0.56 \cdot \%CaCO_3 - 0.7 \cdot \%SO_3) + 1.091 \cdot \%MgO \\ & + 0.71 \cdot \%Na_2O + 0.468(\%K_2O - 0.632 \cdot \%KCl) \end{aligned} \quad (3)$$

The ThCO₂ of the material resulted 23.5%, slightly lower than the total content of calcium registered.

2.2 Carbonation Tests

The slurry carbonation of EAF slag was carried out in a 500 mL flask, using the experimental set-up depicted in Fig. 2. The flask was filled with the slurry (i.e. slag suspended in distilled water, at room temperature) which was homogenized through continuous magnetic stirring. Pure CO₂ was injected continuously into the flask at ambient pressure and at a constant flowrate, which was measured with a flowmeter. The flask was closed with a drilled cap which allows the CO₂ pipe to enter, but the hole was not sealed to avoid the generation of a pressurized system. The experiments were carried out under a suction hood.

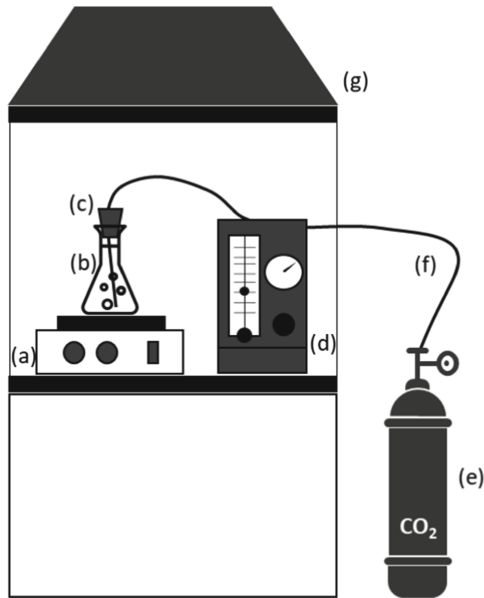


Fig. 2. Experimental set-up: (a) magnetic stirrer; (b) glass flask; (c) drilled cap; (d) flowmeter; (e) CO₂ bottle; (f) polyurethane pipe, Ø 4 mm; (g) aspiration hood.

In this study, all the tests were carried out at room temperature and under a pressure of 1 bar. The slurry was prepared with a L/S of 3, adding 100 g of slag powder to 300 mL

of deionized water. The reaction time was 1 h, the magnetic stirrer was set at 1200 rpm and the CO₂ flowrate was maintained at 150 L/h. The CO₂ partial pressure in the gas cylinder was 99.9%. The pH was measured before and after the carbonation: the initial pH was 11.5 and it decreased to 8 at the end of the experiment.

Three carbonations at the same conditions were repeated to verify the replicability of the experiment. Once concluded the carbonation process, the solid fraction of the slurry was separated from the liquid by centrifugation (REMI), for 4 min at 3000 rpm. Finally, the powder was dried at 60 °C, until the achievement of constant weight.

2.3 Materials Characterization

The dried powder was then analyzed through simultaneous thermogravimetric and differential thermal analysis (TG/DTA, LABSYS EVO from Setaram) in order to quantify the captured CO₂.

The heating process was made by a starting isotherm at 30 °C for 5 min, followed by a heating ramp to 1050 °C, at 10 °C/min, and a cooling step to 30 °C at the same rate. The weight loss attributed to CO₂ decarbonation was determined between 550 °C and 850 °C, according to literature [17–23] and is expressed by Eq. (4).

$$m_{\text{CO}_2}(\%) = \frac{(m_{550\text{ }^\circ\text{C}} - m_{850\text{ }^\circ\text{C}})}{m_i} \cdot 100 \quad (4)$$

where m_i represents the mass of the sample, dried at 60 °C, subjected to thermal treatment. In order to quantify the carbon uptake of the material (%CO₂ uptake), samples were analyzed by TG/DTA before and after the carbonation, using Eq. (5), as proposed by Zhang et al. [24]. The CO₂ uptake, in Eq. (5), represents the carbon content after the carbonation (%CO₂' content) subtracting the initial carbon content from natural carbonates (%CO₂ initial) on the initial weight of the sample. %CO₂' content and %CO₂ initial were calculated with Eq. (4).

$$\% \text{CO}_2 \text{ uptake} \cong \frac{\% \text{CO}'_2 \text{ content} - \% \text{CO}_2 \text{ initial}}{1 - (\% \text{CO}'_2 \text{ content} - \% \text{CO}_2 \text{ initial})} \quad (5)$$

The carbonation performance, denoted as η_{ca} , was defined as the amount of CO₂ actually captured with respect to the theoretical maximum extent of carbonation (Eq. 6).

$$\eta_{ca}(\%) = \frac{\% \text{CO}_2 \text{ uptake}}{\text{ThCO}_2} \cdot 100 \quad (6)$$

XRD analysis were performed on the carbonated powder, in order to detect possible changes in phase compositions. Finally, Scanning Electron Microscopy (SEM, Hitachi, Tokyo, Japan) was used to analyze the powder morphology before and after the carbonation.

3 Results and Discussion

3.1 Composition Analysis of Electric Arc Furnace Slag

Figure 3 shows both the XRD diffraction pattern of raw and carbonated EAF slag. The mineral composition of the untreated material mainly consisted of oxide and silicate phases. In particular, iron and magnesium oxides (FeO , Fe_2MgO_4), aluminosilicates (akermanite and gehlenite) and iron manganese oxide (Fe_2MnO_4) were detected. The same phases were present even after carbonation, indicating that they were not reactive towards CO_2 under the tested conditions. The main crystalline phase identified after the carbonation was calcite, indicating the effective carbonation of the powder. Instead, larnite (Ca_2SiO_4) and merwinite ($\text{Ca}_3\text{MgSi}_2\text{O}_8$), detected in the raw powder, were not determined after the carbonation process, suggesting their participation in the carbonation reaction. The persistence of aluminosilicates, such as akermanite and gehlenite, after the carbonation suggests the possibility to improve the carbonation process efficiency.

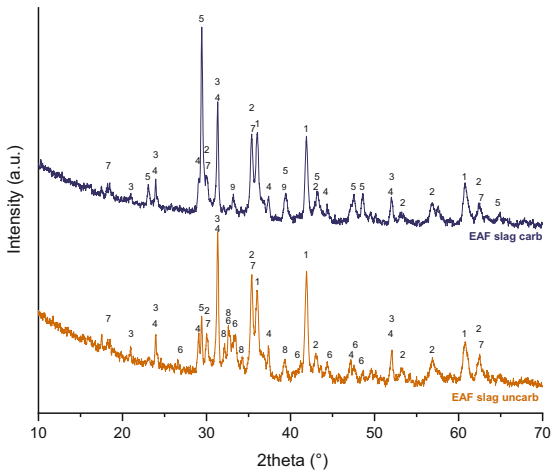


Fig. 3. XRD pattern of raw and carbonated EAF slag. Legend: 1 – Wuestite 96–900-8637 [FeO]; 2 – Magnesioferrite 96–900-3624 [Fe_2MgO_4]; 3 – Akermanite 96–900-6115 [$\text{Ca}_4\text{MgAl}_3\text{SiO}_{14}$]; 4 – Gehlenite 96–101-1003 [$\text{Ca}_2\text{Al}(\text{AlSi})\text{O}_7$]; 5 – Calcium carbonate 00–005-0586 [CaCO_3]; 6 – Merwinite 96–900-0286 [$\text{Ca}_3\text{MgSi}_2\text{O}_8$]; 7 – Fe_2MnO_4 96–230-0619; 8 – Larnite 96–901-2791 [Ca_2SiO_4]; 9 – Hematite 96–101-1268 [Fe_2O_3].

SEM observations (Fig. 4) were performed on both raw (4a, 4c) and treated (4b, 4d) samples, at different magnifications. Although, in the carbonated powder, it was not possible to observe the typical morphologies of calcium carbonate phases [25], some differences can be noted. In fact, the raw particles were characterized by sharp edges with smooth surface, whereas after carbonation the particles appeared to be more rounded with wrinkled surface and several ultrafine surface precipitates.

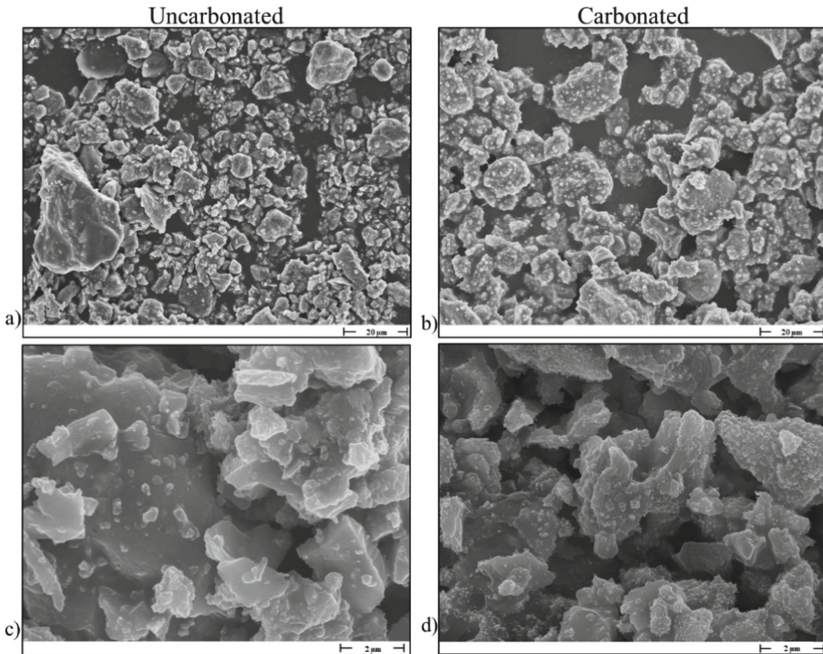


Fig. 4. SEM images of the initial (4a, 4c) and carbonated EAF slag (4b, 4d).

3.2 Thermogravimetric Analysis of Electric Arc Furnace Slag

In Fig. 5, the TG/DTA curve of the raw powder and one representative curve from the three carbonation experiments are reported. To calculate the amount of CaCO_3 , it is necessary to correctly delineate the temperature range in which decomposition takes place, identifying and correcting for possible couplings with other transformations involving mass changes. According to literature, a wide temperature range, between 500 °C and 1000 °C, has been established to refer to the decarbonation process. Specifically, some studies consider the initial decomposition temperature at 500 °C [2, 12, 16, 26–28], while others at 550 °C [17–23]; as final temperature, values of 800 °C [2, 29], 850 °C [12, 16, 18–23, 26, 27] or 1000 °C [17, 28] are considered. These differences can be mainly imputed to chemical purity, defect content, surface area, crystallite size and morphology [30]. In this work, the range between 550 °C and 850 °C has been considered, as the most commonly accepted [17–23], (see dotted lines in Fig. 5) and used to quantify the CO_2 released. As for DTA curves the peaks pointing downwards are associated with endothermic reactions, while those pointing upwards with exothermic phenomena.

According to the TG result, the weight variation of the original sample between 550 °C and 850 °C was not negligible, accounting for 3.4%. The DTA curve of the carbonated sample shows a broad peak below 200 °C that is commonly associated with the formation of calcium silicate hydrates (C-S-H), mainly responsible of the mechanical properties in cement paste. It is worth emphasizing that the mass loss registered due to C-S-H formation is negligible compared to the mass loss due to carbonates decomposition.

For this reason, hydrates contribution was neglected in the formula adopted for the CO₂ uptake assessment (Eq. 5).

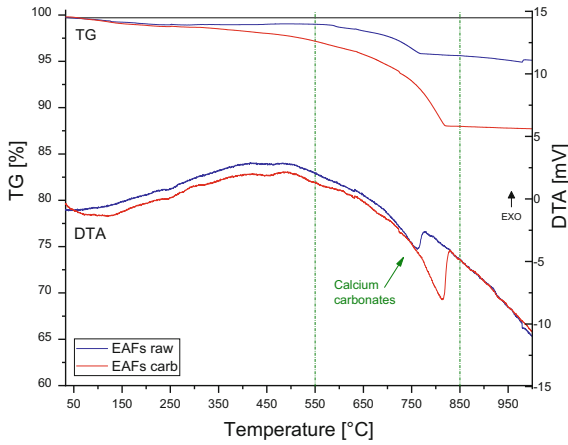


Fig. 5. TGA (black) and DTA (red) curves of raw and carbonated EAF slag.

The results of carbon content obtained from the three carbonated samples were very similar (Fig. 6). The standard deviation of the measured carbon content is 0.31%. As for reproducibility aspects, the low variability of the results, with a coefficient of variation of the measured carbon content equal to 3.27%, emphasises the reliability of the adopted carbonation process. The average final carbon content of the material at the conditions specified in Sect. 2.2 resulted 9.49%, with an average carbon uptake of 6.49% (calculated according to Eq. 5). The carbonation performance (η_a) obtained with these experiments is 27.6% with respect to the theoretical maximum CO₂ uptake (ThCO₂).

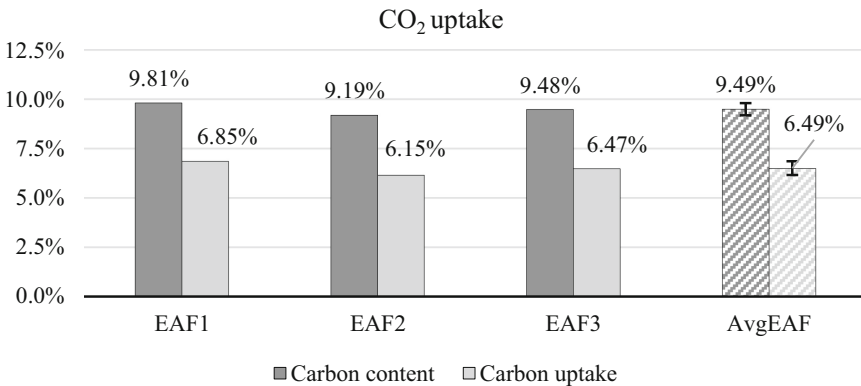


Fig. 6. Comparison of the three experimental results.

Table 2. Summary of the best conditions obtained in this and other studies of wet slurry carbonation of EAF slag.

References	Calcium content [%]	Particle size (μm)	Temperature ($^{\circ}\text{C}$)	Pressure (bar)	Time (h)	L/S	CO ₂ partial pressure	CO ₂ flowrate (L/h)	CO ₂ uptake [%]	Efficiency [%]
Bonenfant et al. (2008) [32]	32.80	106	20	1	24	10	15%	0.3	1.7%	6.6%
Baclocchi et al. (2011) [14]	49.30	105	100	10	4	10	100%	0	14.0%	36.1%
Uibu et al. (2011) [31]	36.12	100	25	1	1.1	10	15%	50	8.7%	30.7%
Uibu et al. (2011) [31]	26.90	100	25	1	1.1	10	15%	50	1.9%	9.0%
Baclocchi et al. (2015) [13]	49.30	150	100	10	24	5	100%	0	28.0%	72.3%
Baclocchi et al. (2015) [13]	49.30	150	100	10	5	5	100%	0	23.0%	59.4%
Omale et al. (2019) [35]	20.90	63	20	5	3	5	100%	0	5.8%	35.6%
Ibrahim (2019)[\diamond] [33]	40.20	250	25	5	6.67	17	10%	42	100.0%	316.6%
Ibrahim (2019) [\diamond] [33]	40.20	250	25	1	15.33	17	10%	42	21.0%	66.5%
This study	27.00	51	25	1	1	3	100%	150	6.7%	31.8%

[\diamond] The slurry solution utilized in these experiments was prepared with seawater at high salinity content.

[*] Calculated according to the equation: $\% \text{CO}_2 \text{ uptake} \cong \frac{\% \text{CO}_2 \text{ content} - \% \text{CO}_2 \text{ initial}}{1 - \% \text{CO}_2 \text{ content}}$

[**] Calculated according to the equation: $\text{Efficiency} = \frac{\% \text{CO}_2 \text{ uptake}}{\% \text{CaO}} \cdot \frac{56}{44} \cdot 100$

3.3 Carbonation Performance

The results can be discussed in comparison with previous literature. Table 2 presents the main results from other studies, each of them determined under the optimized, best conditions, in relation to the slurry carbonation of EAF slag. All the parameters reported in Table 2 have an influence on the carbonation process. The calcium content is typical of the specific material analyzed but can vary in time also from the same production plant. The particle size, in the case of EAF slag, is set during the grinding process. The carbonation performance increases with smaller particle size, but also the energy requirements will increase. Temperature, pressure and time have proved to increase the CO₂ uptake. The CO₂ flowrate is considered equal to zero for all the experiments conducted in closed systems. CO₂ uptake and efficiency (Table 2) are reported based on different equations than the ones proposed in this paper, due to the lack of data. The

results of this study were harmonized and recalculated consequently. Most of the previous literature imposed high temperature or pressure in order to maximize the CO₂ uptake. The results of this study are in line with the other experiments conducted at room temperature and ambient pressure [31, 32]. On the opposite, under the same conditions, a much higher carbonation efficiency (66.5%) was reported by Ibrahim et al. [33]. However, in this previous work, a significantly higher reaction time was employed, and the carbonation was carried out in high-salinity water containing extra Ca and Mg ions, contributing to enhance the carbonation efficiency [34].

4 Conclusions

In this study, slurry carbonation at normal temperature and pressure was conducted on electric arc furnace slag from carbon steel production. The aim is to capture carbon dioxide with an environmentally and economically sustainable process in low energy consumption conditions.

The main outcomes are summarized as follow:

1. The XRD analysis highlighted that larnite is the main compound participating to the carbonation process, while the other calcium aluminosilicates did not react.
2. The repeated experiments obtained a negligible coefficient of variation 3.27%, and it is possible to conclude that the carbonation process is reproducible.
3. The average CO₂ uptake obtained was $6.49 \pm 0.35\%$ and the carbonation performance was 27.6%, a promising result, obtained at room temperature and ambient pressure.
4. The results achieved are in line with previous literature.

Further investigations will focus on the optimization of the process balancing the achievement of higher carbonation efficiencies and the preservation of sustainable carbonation conditions.

References

1. IEA. Cement. <https://www.iea.org/reports/cement>. Accessed 03 Oct 2022
2. Huntzinger, D.N., Gierke, J.S., Sutter, L.L., Kawatra, S.K., Eisele, T.C.: Mineral carbonation for carbon sequestration in cement kiln dust from waste piles. *J Hazard Mater* **168**(1), 31–37 (2009)
3. World Steel in Figures 2022 - worldsteel.org. World Steel Association AISBL. <https://worldsteel.org/steel-topics/statistics/world-steel-in-figures-2022/>. Accessed 03 Oct 2022
4. Worldsteel Association. WORLD STEEL IN FIGURES 2019. <https://worldsteel.org/wp-content/uploads/2019-World-Steel-in-Figures.pdf?x82173>. Accessed 04 Oct 2022
5. EUROSLAG. Statistics 2018. <https://www.euroslag.com/wp-content/uploads/2022/04/Statistics-2018.pdf>. Accessed 04 Oct 2022
6. Piemonti, A., Conforti, A., Cominoli, L., Luciano, A., Plizzari, G., Sorlini, S.: Exploring the potential for steel slags valorisation in an industrial symbiosis perspective at meso-scale level. *Waste Biomass Valorizat.* **1**, 1–21 (2022)
7. European Committee for Standardization. European Standards EN 197-1: 2000 (Amendment A1: 2004): Cement – Part 1: Composition, specifications and conformity criteria for common cements (2004)

8. Huijgen, W.J.J., Comans, R.N.J.: Carbonation of steel slag for CO₂ sequestration: Leaching of products and reaction mechanisms. *Environ. Sci. Technol.* **40**(8), 2790–2796 (2006)
9. Huijgen, W.J.J., Witkamp, G.-J., Comans, R.N.J.: Mineral CO₂ sequestration by steel slag carbonation. *Environ. Sci. Technol.* **39**(24), 9676–9682 (2005)
10. Bobicki, E.R., Liu, Q., Xu, Z., Zeng, H.: Carbon capture and storage using alkaline industrial wastes. *Prog. Energy Combust. Sci.* **38**(2), 302–320 (2012)
11. Song, Q., Guo, M.Z., Wang, L., Ling, T.C.: Use of steel slag as sustainable construction materials: A review of accelerated carbonation treatment. *Resour. Conserv. Recycl.* **173**, 105740 (2021)
12. Chang, E.E., Chen, C.H., Chen, Y.H., Pan, S.Y., Chiang, P.C.: Performance evaluation for carbonation of steel-making slags in a slurry reactor. *J. Hazard. Mater.* **186**(1), 558–564 (2011)
13. Baciocchi, R., et al.: Thin-film versus slurry-phase carbonation of steel slag: CO₂ uptake and effects on mineralogy. *J. Hazard. Mater.* **283**, 302–313 (2015)
14. Baciocchi, R., et al.: Wet versus slurry carbonation of EAF steel slag †. *Greenhouse Gas Sci. Technol.* **1**, 312–319 (2011)
15. Steinour, H.H.: Some effects of carbon dioxide on mortars and concrete-discussion. *J. Am. Concr. Inst.* **30**(2), 905–907 (1959)
16. Huntzinger, D.N., Gierke, J.S., Kawatra, S.K., Eisele, T.C., Sutter, L.L.: Carbon dioxide sequestration in cement kiln dust through mineral carbonation. *Environ. Sci. Technol.* **43**(6), 1986–1992 (2009)
17. Humbert, P.S., Castro-Gomes, J.P., Savastano, H.: Clinker-free CO₂ cured steel slag based binder: Optimal conditions and potential applications. *Constr. Build. Mater.* **210**, 413–421 (2019)
18. Xuan, D., Zhan, B., Poon, C.S., Zheng, W.: Innovative reuse of concrete slurry waste from ready-mixed concrete plants in construction products. *J. Hazard. Mater.* **312**, 65–72 (2016)
19. Liu, G., et al.: Recycling and utilization of high volume converter steel slag into CO₂ activated mortars – The role of slag particle size. *Resour. Conserv. Recycl.* **160**, 104883 (2020)
20. Mahoutian, M., Shao, Y., Mucci, A., Fournier, B.: Carbonation and hydration behavior of EAF and BOF steel slag binders. *Mater. Struct.* **48**(9), 3075–3085 (2014)
21. Moon, E.J., Choi, Y.C.: Development of carbon-capture binder using stainless steel argon oxygen decarburization slag activated by carbonation. *J. Clean. Prod.* **180**, 642–654 (2018)
22. Mo, L., Zhang, F., Deng, M.: Mechanical performance and microstructure of the calcium carbonate binders produced by carbonating steel slag paste under CO₂ curing. *Cem. Concr. Res.* **88**, 217–226 (2016)
23. Mahoutian, M., Chaallal, O., Shao, Y.: Pilot production of steel slag masonry blocks. *Can. J. Civ. Eng.* **45**(7), 537–546 (2018)
24. Zhang, D., Ghoulah, Z., Shao, Y.: Review on carbonation curing of cement-based materials. *J. CO₂ Util* **21**, 119–131 (2017)
25. Ševčík, R., Šašek, P., Viani, A.: Physical and nanomechanical properties of the synthetic anhydrous crystalline CaCO₃ polymorphs: vaterite, aragonite and calcite. *J. Mater. Sci.* **53**(6), 4022–4033 (2018)
26. Chang, E.E., et al.: CO₂ sequestration by carbonation of steelmaking slags in an autoclave reactor. *J. Hazard. Mater.* **195**, 107–114 (2011)
27. Pan, S.Y., Chiang, P.C., Chen, Y.H., Tan, C.S., Chang, E.E.: Kinetics of carbonation reaction of basic oxygen furnace slags in a rotating packed bed using the surface coverage model: Maximization of carbonation conversion. *Appl. Energy* **113**, 267–276 (2014)
28. El Gamal, M., Mohamed, A.-M., Hameedi, S.: Treatment of industrial alkaline solid wastes using carbon dioxide. In: Mateev, M., Nightingale, J. (eds.) *Sustainable Development and Social Responsibility—Volume I*. ASTI, pp. 317–323. Springer, Cham (2020). https://doi.org/10.1007/978-3-030-32922-8_31

29. ben Ghacham, A., Pasquier, L.C., Cecchi, E., Blais, J.F., Mercier, G.: Valorization of waste concrete through CO₂ mineral carbonation: Optimizing parameters and improving reactivity using concrete separation. *J. Clean. Prod.* **166**, 869–878 (2017)
30. Galan, I., Glasser, F.P., Andrade, C.: Calcium carbonate decomposition. *J. Therm. Anal. Calorim.* **111**(2), 1197–1202 (2013)
31. Uibu, M., Kuusik, R., Andreas, L., Kirsimäe, K.: The CO₂ -binding by Ca-Mg-silicates in direct aqueous carbonation of oil shale ash and steel slag. *Energy Proc.* **4**, 925–932 (2011)
32. Bonenfant, D., et al.: CO₂ sequestration potential of steel slags at ambient pressure and temperature. *Ind. Eng. Chem. Res.* **47**(20), 7610–7616 (2008)
33. Ibrahim, M.H., El-Naas, M.H., Zevenhoven, R., Al-Sobhi, S.A.: Enhanced CO₂ capture through reaction with steel-making dust in high salinity water. *Int. J. Greenhouse Gas Control* **91**, 102819 (2019)
34. Wang, W., Liu, X., Wang, P., Zheng, Y., Wang, M.: Enhancement of CO₂ mineralization in Ca²⁺/Mg²⁺-rich aqueous solutions using insoluble amine. *Ind. Eng. Chem. Res.* **52**, 8028–8033 (2013)
35. Omale, S.O., Choong, T.S.Y., Abdullah, L.C., Siajam, S.I., Yip, M.W.: Utilization of Malaysia EAF slags for effective application in direct aqueous sequestration of carbon dioxide under ambient temperature. *Heliyon* **5**(19), e02602 (2019)